JOC Article

The Role of Asynchronous Bond Formation in the Diastereoselective Epoxidation of Cyclic Enol Ethers: A Density Functional Theory Study

Anita M. Orendt,*,‡ Scott W. Roberts,† and Jon D. Rainier*,†

Department of Chemistry, 315 South 1400 East, University of Utah, Salt Lake City, Utah 84112-0850, and Center for High Performance Computing, 155 South 1452 East, University of Utah, Salt Lake City, Utah 84112-0190

rainier@chem.utah.edu; anita.orendt@utah.edu

Received March 7, 2006

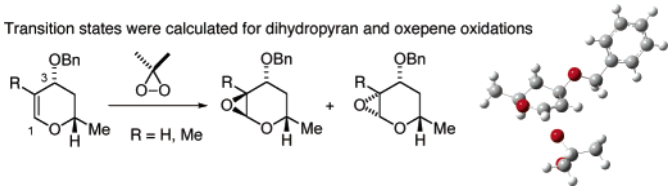

Density functional theory (DFT) (Becke3LYP functional and the D95** basis set) was used to study the influence of substitution on the dimethyldioxirane epoxidation reaction of six- and seven-membered cyclic enol ethers. In agreement with our previously reported experimental results, the calculations predict that substitution on the cyclic enol ether influences the level of diastereoselectivity. Apparent only from the calculations is that the degree of synchronicity in the transition state is important in the diastereoselectivity.

Introduction

Although glycosyl anhydrides have been known since the 1920s,[1] their synthetic potential was not realized until the mid- to late 1980s when it was reported that they could be generated from the reaction of cyclic enol ethers with 3,3-dimethyldioxirane (DMDO).[2] The ability to rapidly and efficiently generate glycosyl anhydrides using DMDO chemistry has had a positive impact on organic and bioorganic chemistry.[3−8]

Our fascination with glycosyl anhydrides results from our interest in using them as intermediates in the chemical synthesis of fused polycyclic ether marine natural products (i.e., gambierol, Figure 1).[9,10]

Central to our approach to this class of targets has been the generation of carbon (*C*)-glycosides and *C*-ketosides from the

† Department of Chemistry.

‡ Center for High Performing Computing.

(1) Brigl, P. *Z. Physiol. Chem.* **1922**, *122*, 245.

(2) (a) Murray, R. W.; Jeyaraman, R. *J. Org. Chem.* **1985**, *50*, 2847. (b) Adam, W.; Bialas, J.; Hadjiarapoglou, L. *Chem. Ber.* **1991**, *124*, 2377.

(3) For a review, see: Danishefsky, S. J.; Bilodeau, M. T. *Angew. Chem., Int. Ed. Engl*. **1996**, *35*, 1380.

(4) For representative examples of DMDO oxidations involving glycals, see: (a) Friesen, R. W.; Sturino, C. F. *J. Org. Chem.* **1990**, *55*, 5808. (b) Gordon, D. M.; Danishefsky, S. J. *J. Org. Chem.* **1991**, *56*, 3713. (c) Murray, R. W.; Shiang, D. L.; Singh, M. *J. Org. Chem.* **1991**, *56*, 3677. (d) Halcomb, R. L.; Wittman, M. D.; Olson, S. H.; Danishefsky, S. J. *J. Am. Chem. Soc.* **1991**, *113*, 5080. (e) Berkowitz, D. B.; Danishefsky, S. J.; Schulte, G, K. *J. Am. Chem. Soc.* **1992**, *114*, 4518. (f) Link, J. T.; Gallant, M.; Danishefsky, S. J. *J. Am. Chem. Soc.* **1993**, *115*, 3782. (g) Randolph, J. T.; Danishefsky, S. J. *J. Am. Chem. Soc.* **1995**, *117*, 5693. (h) Flaherty, T. M.; Gervay, J. *Tetrahedron Lett.* **1996**, *37*, 961. (i) Lee, G. S.; Min, H. K.; Chung, B. Y. *Tetrahedron Lett.* **1999**, *40*, 543. (j) Upreti, M.; Ruhela, D.; Vishwakarma, R. A. *Tetrahedron*, **2000**, *56*, 6584. (k) Chiara, J. L.; Sesmilo, E. *Angew. Chem., Int. Ed*. **2002**, *41*, 3242. (l) Demange, R.; Awad, L.; Vogel; P. *Tetrahedron: Asymmetry* **2004**, *15*, 3573.

(5) For representative examples of DMDO oxidations of enol ethers in natural product synthesis, see: (a) Adam, W.; Golsch, D.; Hadjiarapoglou, L.; Patonay, T. *J. Org. Chem*. **1991**, *56*, 7292. (b) Hayward, M. M.; Roth, R. M.; Duffy, K. J.; Dalko, P. I.; Stevens, K. L.; Guo, J.; Kishi, Y. *Angew. Chem., Int. Ed*. **1998**, *37*, 190. (c) Evans, D. A.; Trotter, B. W.; Cote, B. *Tetrahedron Lett*. **1998**, *39*, 1709. (d) Rainier, J. D.; Allwein, S. P.; Cox, J. M. *J. Org. Chem.* **2001**, *66*, 1380. (e) Hale, K. J.; Frigerio, M.; Manaviazar, S. *Org. Lett*. **2003**, *5*, 503.(f) Johnson, H. W. B.; Majumder, U.; Rainier, J. D. *J. Am. Chem. Soc.* **2005**, *127*, 848.

(6) For DMDO oxidations of glycals on solid support, see: Randolf, J. T.; McClure, K. F.; Danishefsky, S. J. *J. Am. Chem. Soc*. **1995**, *117*, 5712.

(7) For DMDO oxidations of oxepenes to create septanose carbohydrates, see: ref 11b. And: (a) Peczuh, M. W.; Snyder, N. L.; Fyvie, W. S. *Carbohydr. Res*. **2004**, *339*, 1163. (b) DeMatteo, M. P.; Snyder, N. M.; Morton, M.; Baldisseri, D. M.; Hadad, C. M.; Peczuh, M. W. *J. Org. Chem.* **2005**, *70*, 24.

(8) Halcomb, R. L.; Danishefsky, S. J. *J. Am. Chem. Soc.* **1989**, *111*, 6661.

(9) For recent reviews describing the synthesis of polycyclic ethers see: (a) Inoue, M. *Chem. Rev*. **2005**, *105*, 4379. (b) Nakata, T. *Chem. Rev.* **2005**, *105*, 4314.

(10) For the isolation and structure elucidation of gambierol see: (a) Satake, M.; Murata, M.; Yasumoto, T. *J. Am. Chem. Soc*. **1993**, *115*, 361. (b) Morohashi, A.; Satake, M.; Yasumoto, T. *Tetrahedron Lett.* **1998**, *39*, 97.

10.1021/jo060502g CCC: $33.50
Published on Web 06/20/2006

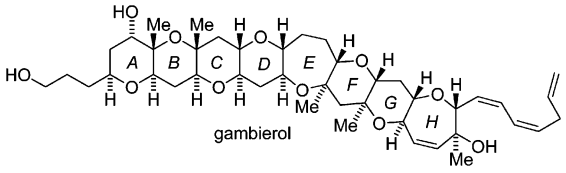

FIGURE 1. Structure of gambierol.

SCHEME 1

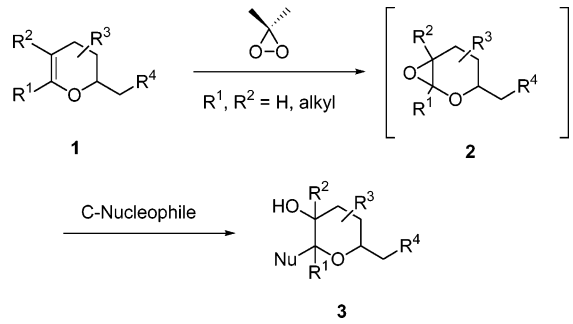

coupling of *C*-nucleophiles with DMDO generated anhydrides (Scheme 1).[11]

Critical to the success of this approach is that the oxidation reaction be stereoselective. Because the conditions used in reagent controlled asymmetric oxidation reactions are incompatible with most glycosyl anhydrides,[12] the vast majority of work in this area has focused on the use of the substrate to control the facial selectivity in the oxidation. With this in mind, the best-studied substrate in the DMDO oxidation of dihydropyrans has been trisbenzylidene-D-glucal (**4**).[8] In our hands, the DMDO oxidation of **4** gave a 20:1 mixture of diastereomers favoring the expected isomer **5**, where DMDO had oxidized the alkene from the face opposite the C(3) benzyl ether (eq 1).[13]

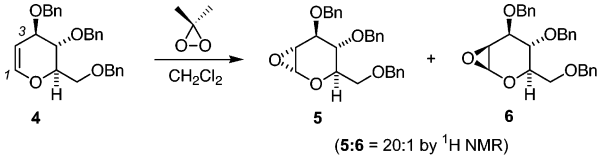

(1)

Even higher levels of selectivity were observed with substrates lacking the C(4) substituent. For example, the oxidation of **7** gave anhydride **8** as the only product observed by ^{13}C NMR (eq 2).[14]

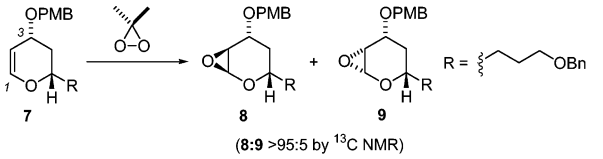

(2)

We have noted that alkyl substitution at C(2) has a dramatic effect on selectivity. In the course of our total synthesis of the marine ladder toxin gambierol,[5f] the diastereoselectivity deteriorated to 8:1 when dihydropyran **10** was oxidized with DMDO.[15,16]

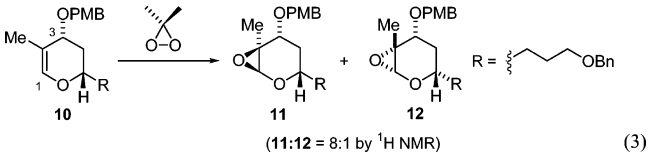

(3)

In the course of our synthetic efforts, we have also had the opportunity to study the oxidation of α-substituted and α-unsubstituted oxepenes and have found that α-substituted oxepenes generally give high levels of selectivity while α-unsubstituted oxepenes are less selective.[11b,14] Three examples from our laboratories best illustrate these phenomenon. The first was critical for the generation of the gambierol H-ring. When oxepene **13** was treated with DMDO followed by DIBAl-H, alcohol **14** was isolated in 90% yield as a single diastereomer.[14]

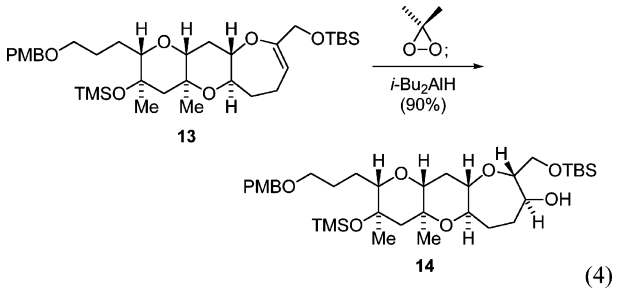

(4)

The second also comes from our gambierol work. When oxepene **15** was sequentially exposed to DMDO and DIBAl-H, we isolated a 10:1 mixture of 2° alcohols **17** in 90% yield.[5f,17] Surprising was that the major anhydride diastereomer from the DMDO reaction was **16** resulting from the reaction of DMDO on the same face of **15** as the C(21) angular methyl group.

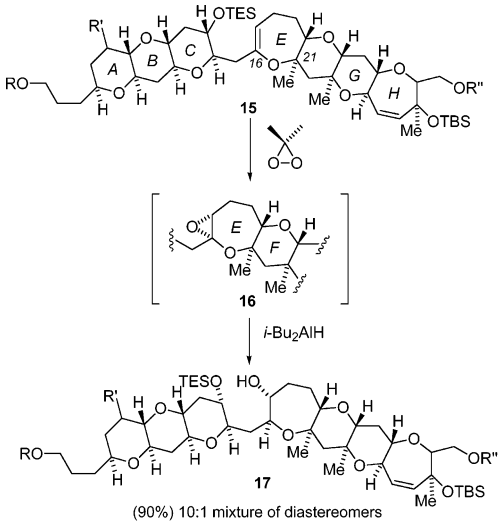

(5)

(11) (a) Rainier, J. D.; Allwein, S. P. *J. Org. Chem.* **1998**, *63*, 5310. (b) Allwein, S. P.; Cox, J. M.; Howard, B. E.; Johnson, H. W. B.; Rainier, J. D. *Tetrahedron* **2002**, *58*, 1997.

(12) With the exception of acylated substrates, glycosyl anhydrides undergo epoxide opening under the biphasic conditions used in asymmetric epoxidation chemistry. See: Chan, W.-K.; Wong, M.-K.; Che, C.-M. *J. Org. Chem.* **2005**, *70*, 4226.

(13) The subsequent coupling of **5** with propenylmagnesium chloride results in the generation of the corresponding *β*-*C*-glycoside in 83% yield. See: ref 11.

(14) The subsequent coupling of **8** with propenylmagnesium chloride resulted in the generation of the corresponding *β*-*C*-glycoside in 95% yield. See: Majumder, U.; Cox, J. M.; Johnson, H. W. B.; Rainier, J. D. *Chem. Eur. J.* **2006**, *12*, 1736.

As an example of a relatively unselective oxidation reaction of α-unsubstituted oxepenes, exposure of **18** to DMDO gave a 2:1 mixture of anhydrides **19** as measured by ^{1}H NMR.[18] We subsequently showed that **19** underwent an efficient coupling with propenylmagnesium chloride to give the corresponding allyl substituted product.

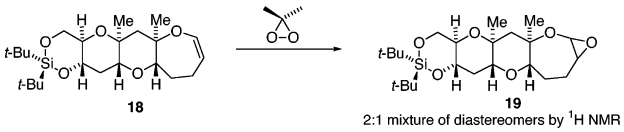

(6)

In contrast to the oxidation of **13**, **15**, and **18** with DMDO, the oxidations of related cycloheptenyl substrates with *m*-chloroperbenzoic acid (*m*-CPBA) have been found to be stereoselective and to occur from the face of the molecule opposite the angular methyl substituent (eq 7).[19]

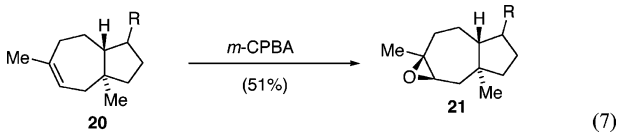

(7)

To get a better sense of the experimental observations outlined above, we decided to study the epoxide forming reactions computationally. A number of epoxidation transition states have been computed at many different levels of theory ranging from semiempirical to higher levels including MP2, CCSD, and CASSCF.[20] The majority of work in this area has focused on the structure of the transition state and whether the process occurs via the synchronous formation of the two C−O bonds or via an unsymmetrical, asynchronous mechanism. As such, the consensus is that the transition state almost always takes a "spiro" butterfly structure and that the transition state is symmetrical or synchronous when the alkene is symmetrically substituted and unsymmetrical or asynchronous otherwise.[21]

Two differences distinguish the reactions of interest to us from those examined previously: First, our substrates are more complex than the majority of others that have been studied. Among the more architecturally complex substrates that have been examined to date using ab initio or semiempirical methods have been substituted dihydronaphthalenes and norbornenes. The dihydronaphthalene work was carried out by Lucero and Houk and studied at the PM3 semiempirical level.[22] They concluded that the experimentally derived diastereoselectivity for the epoxidation of dihydronaphthalene derivatives resulted from developing torsional strain between the forming C−O bonds and the axial C−H bond on the allylic carbon atoms. Norbornene oxidations have been examined in two independent studies. Sarzi-Amadi et al. invoked a torsional strain argument to interpret the computed diastereoselectivity for the epoxidation of norbornene derivatives and cyclohexenol.[23] Bach et al. calculated the approach of oxidizing agents, including DMDO, to the *exo* and *endo* faces of norbornene and benzonorbornadiene.[24] As expected, they found the *exo* approach to be favored with these substrates.

The second difference with our substrates is that the olefins are contained in cyclic enol ethers. Despite the aforementioned importance of cyclic enol ether oxidations, there is currently no firm understanding of the features responsible for diastereoselectivity.[25]

With the preceding as background, we decided to determine whether density functional theory (DFT) calculations using the B3LYP hybrid could help us to better understand some of the interesting experimental observations listed above. The results of these calculations are contained herein.

Method of Calculation

Although there have been recent reports questioning the accuracy of the B3LYP method in asynchronous reactions,[26] its use has been validated in independent studies by Bach, Singleton, and Houk.[25b,27,28] Thus, although the activation barriers are generally overestimated relative to higher levels of theory, we decided to employ DFT and the B3LYP method in our studies. All calculations including transition-state geometries were completed using the Gaussian03 package, version C.01.[29] Geometry optimizations of the starting materials, and the epoxidation products were completed using the B3LYP hybrid functional as specified in Gaussian03[30] and the D95** basis set.[31] The transition states were checked to confirm that they corresponded to the epoxidation reaction by completing a frequency calculation and visually observing that the normal mode of the imaginary frequency corresponded to the reaction. In addition, intrinsic reaction coordinate (IRC) calculations[32] were completed in both directions (from the transition state to both starting material and products) on all transition states reported. In these calculations, either eight or twelve points were completed in each direction, using the default step size in Gaussian03.

(15) Cox, J. M.; Rainier, J. D. *Org. Lett.* **2001**, *3*, 2919.

(16) The subsequent coupling of the mixture of **11** and **12** with propenylmagnesium chloride resulted in the generation of the corresponding *β-C*-glycosides in 90% yield. See: ref 14.

(17) Johnson, H. W. B.; Majumder, U.; Rainier, J. D. *Chem. Eur. J.* **2006**, *12*, 1747.

(18) Roberts, S.; Rainier, J. D. Unpublished results.

(19) Nakashima, K.; Inoue, K.; Sono, M.; Tori, M. *J. Org. Chem.* **2002**, *67*, 6034.

(20) (a) Singleton, D. A.; Wang, Z. H. *J. Am. Chem. Soc.* **2005**, *127*, 6679. (b) Freccero, M.; Gandolfi, R.; Sarzi-Amade, M.; Rastelli, A. *J. Org. Chem.* **2004**, *69*, 7479. (c) Okovytyy, S.; Leszczynski, J. *Tetrahedron Lett.* **2002**, *43*, 4215. (d) Deubel, D. V. *J. Org. Chem.* **2001**, *66*, 3790. (e) Washington, Y.; Houk, H. N. *Angew. Chem., Int. Ed.* **2001**, *40*, 4485. (f) Chekroun, A.; Jarid, A.; Benharref, A.; Boutalib, A. *J. Org. Chem.* **2000**, *65*, 4431. (g) Freccero, M.; Gandolfi, R.; Sarzi-Amade, M.; Rastelli, A. *J. Org. Chem.* **2000**, *65*, 2030. (h) Manoharan, M. *J. Org. Chem.* **2000**, *65*, 1093. (i) Freccero, M.; Gandolfi, R.; Sarzi-Amade, M. *Tetrahedron* **1999**, *55*, 11309. (j) Bach, R. D. Glukhovtsev, M. N.; Gonzales, C. *J. Am. Chem. Soc.* **1998**, *120*, 9902, and references therein. (k) Freccero, M.; Gandolfi, R.; Sarzi-Amade, M.; Rastelli, A. *Tetrahedron* **1998**, *22*, 6123. (l) Miaskiewics, K.; Smith, D. A. *J. Am. Chem. Soc.* **1998**, *120*, 1872. (m) Bach, R. D.; Glukovtsev, M. N.; Canepa, C. *J. Am. Chem. Soc.* **1998**, *120*, 775. (n) Singleton, D. A.; Merrigan, S. R.; Liu, J.; Houk, K. N. *J. Am. Chem. Soc.* **1997**, *119*, 3385. (o) Houk, K. N.; Liu, J.; DeMello, N. C.; Condroski, K. R. *J. Am. Chem. Soc.* **1997**, *119*, 10147, and references therein.

(21) Bartlett, P. D. *Rec. Chem. Prog.* **1950**, *11*, 47.

(22) Lucero, M. J.; Houk, K. N. *J. Org. Chem.* **1998**, *62*, 66973.

(23) Freccero, M.; Gandolfi, R.; Sarzi-Amade, M.; Rastelli, A. *J. Org. Chem.* **2002**, *67*, 8519. (b) Freccero, M.; Gandolfi, R.; Sarzi-Amade, M.; Rastelli, A. *J. Org. Chem.* **2000**, *65*, 8948.

(24) Bach, R. D.; Dmitrenko, O.; Adam, W.; Schambony, S. *J. Am. Chem. Soc.* **2003**, *125*, 924.

(25) Houk has calculated the transition structure for the DMDO oxidation of methylvinyl ether and the enol acetate of cyclopentanone derivatives. See: (a) Houk, K. N.; Liu, J.; DeMello, N. C.; Condroski, K. R. *J. Am. Chem. Soc.* **1997**, *119*, 10147. (b) Cheong, P. H.-Y.; Yun, H.; Danishefsky, S. J.; Houk, K. N. *Org. Lett.* **2006**, *8*, 1513.

(26) (a) Okovytyy, S.; Gorb, L.; Leszczynski, J. *Tetrahedron Lett.* **2002**, *43*, 4215. (b) Carlier, P. R.; Deora, N.; Crawford, T. D. *J. Org. Chem.* **2006**, *71*, 1592.

(27) (a) Bach, R. D.; Glukhovtsev, M. N.; Gonzales, C.; Marquez, M.; Estevez, C. M. Baboul, A. G.; Schlegel, H. B. *J. Phys. Chem. A* **1997**, *101*, 6092. (b) Bach, R. D.; Dmitrenko, O. *J. Phys. Chem. A* **2003**, *107*, 4300. (c) Dmitrenko, O.; Bach, R. D. *J. Phys. Chem. A* **2004**, *108*, 6886.

(28) Singleton, D. A.; Wang, Z. *J. Am. Chem. Soc.* **2005**, *127*, 6679.

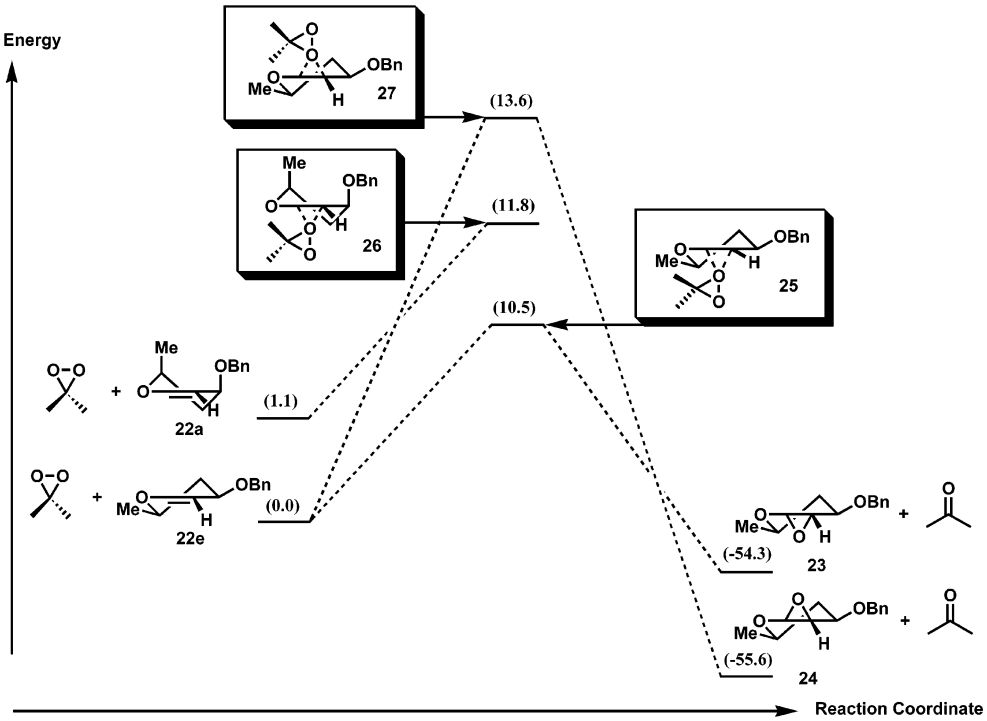

FIGURE 2. Free energy diagram for the reaction of **22** with DMDO.

Results and Discussion

We first calculated the transition states for the oxidation of disubstituted dihydropyran **22** (eq 8). Attack from the face of **22** opposite the C(3) benzyl ether would give the *anti*-product **23**, while attack from the face of the benzyl ether would give the *syn*-product **24**.[33]

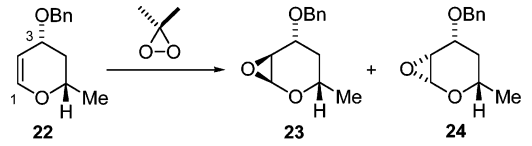

(8)

The computed ground-state conformations for disubstituted dihydropyran **22** are shown in eq 9. Not surprising was that the favored conformer had both the methyl and benzyl ethers oriented in the pseudoequatorial positions.[34]

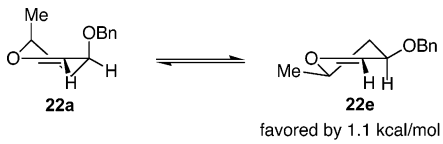

(9)

Three transition structures were found for the oxidation of **22** with DMDO (Figure 2): one had DMDO approach syn to the C(3) benzyl ether (i.e. **27**) and two had it approaching anti (i.e., **25** and **26**).[35]

The formation of the C−O bonds of the anhydride was unsymmetrical; bond formation at C(2) preceded bond formation at C(1) by 0.38 Å in **25**, 0.42 Å in **26**, and 0.26 Å in **27** (Figure 3). Related to this was that the transition structures showed considerable oxocarbenium ion character, as evidenced by a shortening of the C(1)−pyranyl oxygen bond during the transition to the anhydride (see Table 1). *Anti*-structures **25** and **26** differed from one another in the conformation of the pyran ring. The higher energy of the two (i.e., **26**) had the methyl and benzyl ether substituents oriented in pseudoaxial positions,

(29) Frisch, M. J.; Trucks, G. W.; Schlegel, H. B.; Scuseria, G. E.; Robb, M. A.; Cheeseman, J. R.; Montgomery, J. A., Jr.; Vreven, T.; Kudin, K. N.; Burant, J. C.; Millam, J. M.; Iyengar, S. S.; Tomasi, J. ; Barone, V.; Mennucci, B.; Cossi, M.; Scalmani, G.; Rega, N.; Petersson, G. A.; Nakatsuji, H.; Hada, M.; Ehara, M.; Toyota, K.; Fukuda, R.; Hasegawa, J.; Ishida, M.; Nakajima, T.; Honda, Y.; Kitao, O.; Nakai, H.; Klene, M.; Li, X.; Knox, J. E.; Hratchian, H. P.; Cross, J. B.; Bakken, V.; Adamo, C.; Jaramillo, J.; Gomperts, V; Stratmann, R. E.; Yazyev, O.; Austin, A. J.; Cammi, R.; Pomelli, C.; Ochterski, J. W.; Ayala, P. Y.; Morokuma, K.; Voth, G. A.; Salvador, P.; Dannenberg, J. J.; Zakrzewski, V. G.; Dapprich, S.; Daniels, A. D.; Strain, M. C.; Farkas, O.; Malick, D. K.; Rabuck, A. D.; Raghavachari, K.; Foresman, J. B.; Ortiz, J. V.; Cui, Q.; Baboul, A. G.; Clifford, S.; Cioslowski, J.; Stefanov, B. B.; Liu, G.; Liashenko, A.; Piskorz, P.; Komaromi, I.; Martin, R. L.; Fox, D. J.; Keith, T.; Al-Laham, M. A.; Peng, C. Y.; Nanayakkara, A.; Challacombe, M.; Gill, P. M. W.; Johnson, B.; Chen, W.; Wong, M. W.; Gonzalez, C.; Pople, J. A. *Gaussian 03*, Revision C.01; Gaussian, Inc.: Wallingford CT, 2004.

(30) Becke, A. D. *J. Chem. Phys.* **1993**, *98*, 5648. (b) Lee, C.; Yang, W.; Parr, R. G. *Phys. Rev. B* **1988**, *37*, 785. (c) Stevens, P. J.; Devlin, F. J.; Chabalowski, C. F.; Frisch, M. J. *J. Phys. Chem.* **1994**, *98*, 11623.

(31) Dunning, T. H., Jr.; Hay, P. J. In *Modern Theoretical Chemistry*; Schaefer, H. F., III, Ed.; Plenum: New York, 1976; Vol. 3, pp 1−28.

(32) Gonzales, C.; Schlegel, H. B. *J. Chem. Phys.* **1989**, *90*, 2154. (b) Gonzales, C.; Schlegel, H. B. *J. Phys. Chem.* **1990**, *94*, 5523.

(33) These calculations were also performed with a methyl ether at the C(3) position to determine if the large benzyl group was responsible for any systematic error. The Gibb's free energy profile for the C(3) methyl ether was virtually identical to the data presented for the C(3) benzyl ether substrate.

(34) Replacement of the C(5) methyl group in **22** with hydrogen resulted in the ground-state conformer having the benzyl ether oriented in the axial position as the lowest energy conformer. For a discussion of the influence of electronegative atoms on the conformations of cyclohexenes. See: Eliel, E. L. *Stereochemistry of Organic Compounds*; John Wiley & Sons: New York, 1994; p 727.

(35) The transition state corresponding to DMDO approaching **22a** syn-to the axial C_3−OBn ether was ruled out as being improbable on the basis of steric considerations.

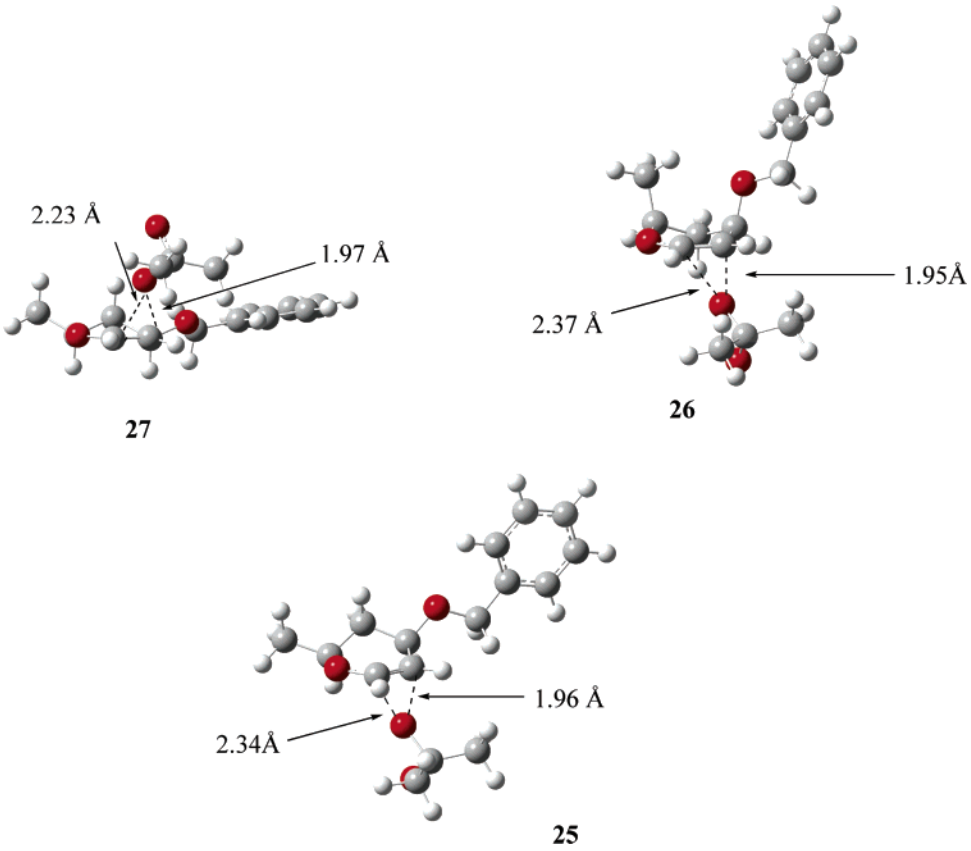

FIGURE 3. Calculated transition structures for the reaction of **22** with DMDO.

while the more stable (i.e., **25**) had them oriented in pseudoequatorial positions.[36] Interesting was that **25** was the low-energy transition structure despite the eclipsing interactions between the C(2)−O and C(3) C−H bonds and its twist boat conformation. The implication is that 1,3-diaxial interactions in **26** were more energetically unfavorable than the developing torsional strain in **25**. On the other hand, having the substituents oriented axially in **26** was less unfavorable than having DMDO approach syn to the C(3) benzyl ether as in **27**.

A consequence of the unsymmetrical nature of C−O bond formation is that DMDO is shifted toward the C(3) substituent, resulting in increased interactions between it and the benzyl ether in the *syn*-transition structure **25**.[37] Consistent with this is that the oxidation of cyclohexenyl substrates that are analogous to **4**, **7**, and **10** are much less stereoselective. Ganem found that the *m*-CPBA oxidation of cyclohexene **28** gave **29** as a 2.5:1 mixture of diastereomers.[38]

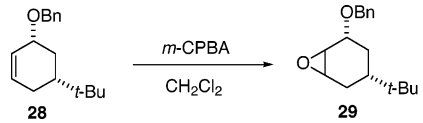

(10)

Having computed transition structures for the reaction of dihydropyran **22** with DMDO, we next explored the oxidation of C(2)-substituted dihydropyran **30** (eq 11).

As with **22**, we initially calculated ground-state conformations and found the conformer having the substituents oriented in the pseudoequatorial positions (i.e., **30e**) to again be favored. On the basis of the presence of $A_{1,2}$ strain between the C(2) and

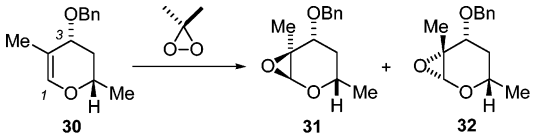

(11)

C(3) substituents, it was not surprising that the difference in energy between the two conformers was lower by 0.3 kcal/mol in **30** than it had been in **22**.[39]

(12)

Also consistent with **22** was that three transition structures (**33**, **34**, and **35**) were found for the oxidation of **30** (Figure 4). Consistent with our experimental data, the two *anti*-transition structures **33** and **34** were lower in energy than the *syn*-structure **35**. Although the calculations overestimate the magnitude of

(36) The low-energy transition structure for the dihydropyran lacking the C(5) methyl substituent corresponded to **26** having the benzyl ether oriented in the axial direction.

(37) Houk has proposed a similar "tilting away" from the more substituted carbon of the olefin; see: ref 20o.

(38) (a) McKittrick, B. A.; Ganem, B. *Tetrahedron Lett.* **1985**, *26*, 4895. Ogawa and co-workers have observed a similar phenomenon; see: (b) Ogawa, S.; Watanabe, M.; Maruyama, A.; Hisamatsu, S. *Bioorg. Med. Chem. Lett.* **2002**, *12*, 749.

(39) For a discussion of allylic strain, see: Eliel, E. L.; Wilen, S. H. *Stereochemistry of Organic Compounds*; John Wiley & Sons: New York, 1994; p 738.

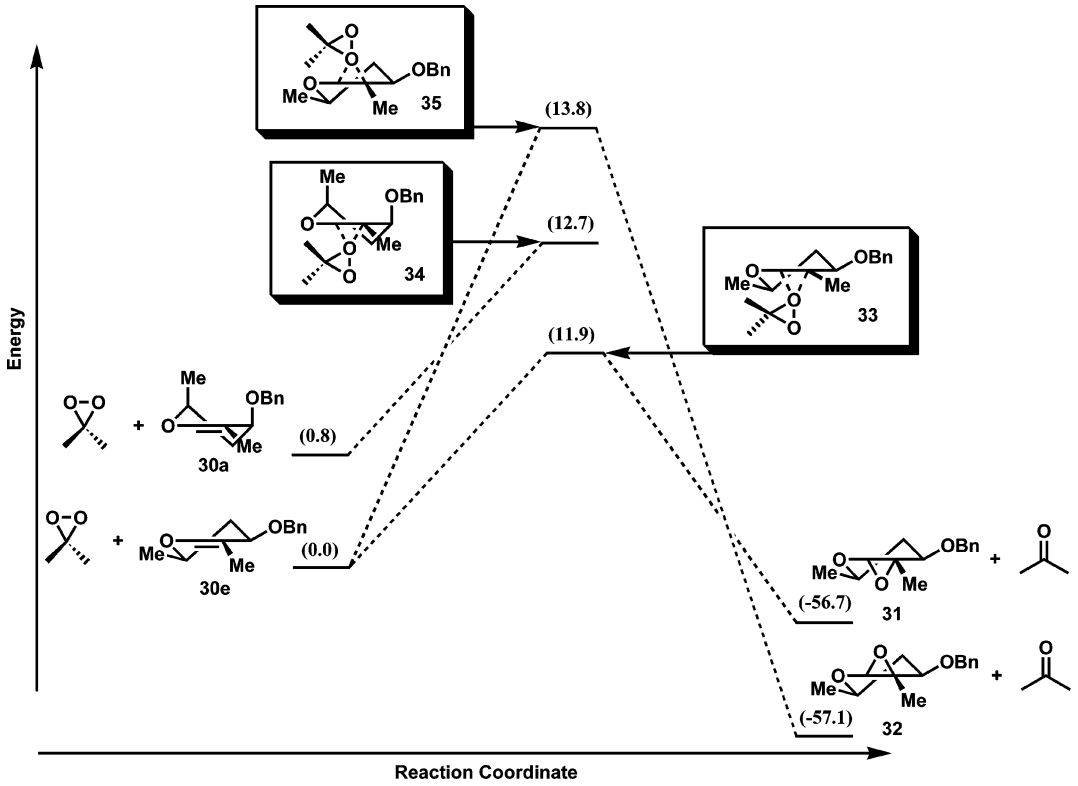

FIGURE 4. Free energy diagram for the reaction of **30** with DMDO.

TABLE 1. Calculated Bond Lengths for 24−29 (Å)

substrate	O_{pyran}−C(1)	C(1)−C(2)	C(2)−C(3)	C(1)−O_{DMDO}	C(2)−O_{DMDO}	O−O
22e	1.36	1.34	1.51			
22a	1.36	1.35	1.50			
23	1.38	1.48	1.53	1.43	1.46	
24	1.38	1.49	1.52	1.43	1.45	
25	1.33	1.38	1.52	2.34	1.96	1.87
26	1.32	1.38	1.51	2.37	1.96	1.87
27	1.33	1.38	1.51	2.23	1.97	1.88

the difference in energy between the two substrates, they are consistent with our experimental trends for **10** (eq 3), where *β*-methyl substitution negatively affects diastereoselectivity.[40] The difference in energy between the low-energy *anti*-transition structure and the *syn*-transition structure was lower for the oxidation of **30** than it had been for **22** (3.1 kcal/mol for **22** vs 1.9 kcal/mol for **30**).

There were similarities and notable differences between the transition structures for the oxidations of **30** and **22** (Figure 5). Similarities included the conformations of the transition states. For example, the favored structure for the oxidation of **30** (i.e., **33**) resembled a twist boat where developing torsional strain between the C(3) C−O bond and the C(3) C−H bond does not prohibit it from being the low-energy conformer. The most significant differences centered on bond lengths. Due to the opposing charge stabilization of the C(2) methyl group and the pyranyl oxygen, the C(1) and C(2) C−O bond lengths were much more synchronous in **30** than they had been for **22**. As can be seen by comparing the data in Tables 1 and 2, the C(2) C−O bond length preceded the C(1) C−O bond length by 0.12 and 0.38 Å for the most favored *anti*-structures **33** and **25**, respectively, and 0.01 and 0.26 Å for the high-energy *syn*-structures **35** and **27**, respectively.

We believe that the diminished selectivity observed for **30** with respect to **22** is a result of both the stabilization of the *syn*-transition state **35** and the destabilization of the *anti*-structures **33** and **34**. The stabilization of **35** is the result of the aforementioned more symmetrical C−O bond formation and, as a result, the diminished interactions between DMDO and the C(3) benzyl ether. The destabilization of **33** and **34** is a result of torsional strain between the C(2) methyl group and the C(3) benzyl ether as DMDO approaches **30** anti to the benzyl ether. Consistent with this argument is that the difference in energy between the low and higher energy *anti*-transition structures **33** and **34**, respectively, is also diminished in **30** when compared to **22** (1.4 kcal/mol in **22** vs 0.8 kcal/mol in **30**) since the developing torsional strain between the benzyl ether and methyl group should be more pronounced in **33** when compared to **34** (i.e., the dihedral angle between the methyl group and the benzyl ether is smaller for **33** than it is for **34**; see Table 3).

Oxepenes

Having calculated transition structures for the dihydropyran oxidations that agree with our experimental data, we next computed transition structures for the DMDO reactions of

(40) The experimentally derived ratio of 8:1 corresponds to an energy difference of 1.23 kcal at 0 °C.

TABLE 2. Calculated Bond Lengths for 30−35 (Å)

substrate	O_{pyran}−C(1)	C(1)−C(2)	C(2)−C(3)	C(1)−O_{DMDO}	C(2)−O_{DMDO}	O−O
30e	1.37	1.35	1.51			
30a	1.36	1.35	1.50			
31	1.38	1.48	1.54	1.43	1.47	
32	1.38	1.48	1.53	1.43	1.46	
33	1.33	1.39	1.53	2.16	2.04	1.91
34	1.32	1.39	1.51	2.21	2.02	1.89
35	1.33	1.39	1.51	2.09	2.08	1.89

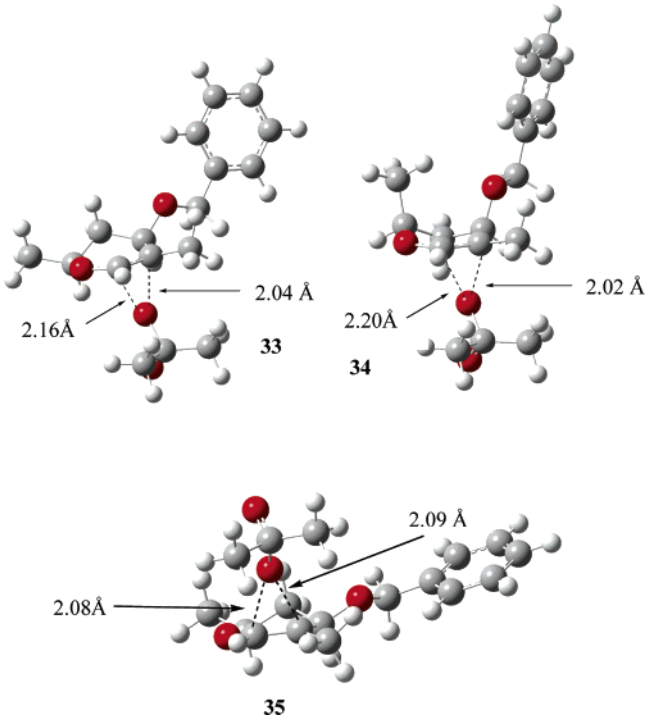

FIGURE 5. Transition structures for the reaction of **30** with DMDO.

TABLE 3. C(2)−CH_3 and the C(3)−OBn Dihedral Angles (deg) for 33, 34, and 35

TS	C(2)−CH_3 to C(3)−OBn	C(2)−CH_3 to C(3)−H
33	31	89
34	59	58
35	44	73

α-substituted and α-unsubstituted oxepenes **36** and **37**, respectively (eq 13).

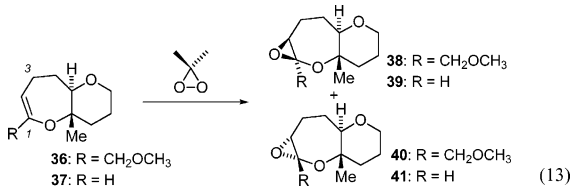

(13)

Although the magnitudes of the energy differences were overestimated (Figure 6), once again the calculations were consistent with our experimental observations. They predicted that the formation of the anhydride from the side of the angular methyl group was favored with both **36** and **37** and that the reaction of **36** with DMDO should be more selective than the same reaction with **37**.

In all four transition structures (Figure 7), the C(2) C−O bonds were much shorter than the C(1) C−O bonds, dioxirane approached the enol ether in a spiro-fashion, and the oxepenes adopted pseudo-chair conformations.

TABLE 4. Dihedral Angles (deg) between DMDO and the Allylic H's during the Oxidation of Oxepenes 36 and 37

TS	C(2)−O(DMDO) to C(3)−H_{ax}	C(2)−O(DMDO) to C(3)−H_{eq}
42	176	62
43	175	61
44	36	108
45	34	148

Consistent with our results with the dihydropyrans, we believe that the asynchronous nature of the forming C−O bonds is an important factor in the selectivity of oxepenes **36** and **37**. From an examination of the transition structures, we believe that the important interactions in these oxidations are those between DMDO and the allylic C−H bonds.[41] In the disfavored transition states **44** and **45**, the C(2)−O bond nearly eclipses the axial allylic C(3)−H bond (dihedral angle = 36°; see Table 4). In contrast, DMDO approaches the alkene in transition structures **42** and **43** from the pseudoaxial direction with all bonds staggered. That DMDO is shifted toward C(2) has a second effect: unfavorable nonbonded interactions between DMDO and the angular methyl group as DMDO approaches the alkene are alleviated. This analysis is consistent with the selectivity seen with cycloheptene **20** (eq 7), where the angular methyl group dictated the facial selectivity in the oxidation reaction. One would predict that C−O bond formation would be much more symmetrical with this substrate and that the interactions between DMDO and the methyl group in the transition state would be important.

Although the relatively large (2 kcal/mol) difference in energy between the α-substituted and α-unsubstituted oxepene transition states **42** and **43**, respectively, is difficult to rationalize in light of the similarities in their bond lengths, there is precedent for similar differences leading to analogous energies. Houk has observed that the B3LYP/6-31G* computed transition state for the reaction of dioxirane with propylene was stabilized by 2 kcal/mol when compared to the transition state for the same reaction with ethylene; the C−O bonds in the propylene transition structure were found to be more asynchronous than those in the ethylene structure by 0.14 Å.[20o] Based on this, we propose that the differences observed both experimentally and computationally between the α-substituted and the α-unsubstituted oxepenes **36** and **37**, respectively, are a reflection of their respective substitution patterns. That the correlation between the differences in C−O bond lengths (0.1 Å) and energy (2 kcal/mol) between **42** and **43** is nearly identical to that found by Houk in much simpler systems is interesting.

(41) See: refs 22 and 25b. And: Ando, K.; Green, N. S.; Li, Y.; Houk, K. N. *J. Am. Chem. Soc.* **1999**, *121*, 5334, and references therein.

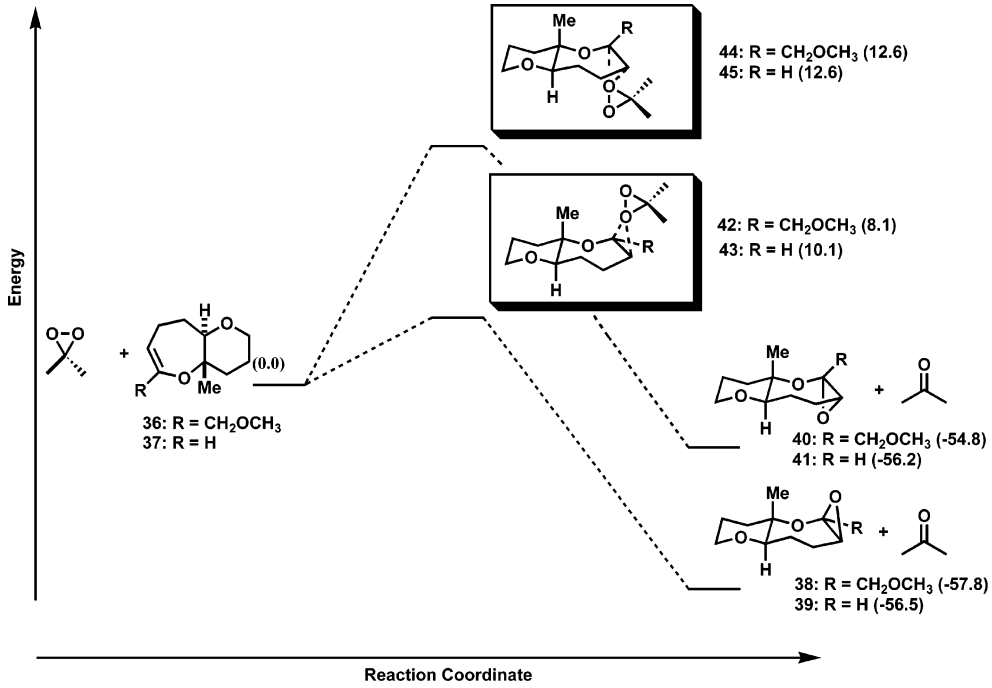

FIGURE 6. Free energy diagram for the reaction of **36** and **37** with DMDO.

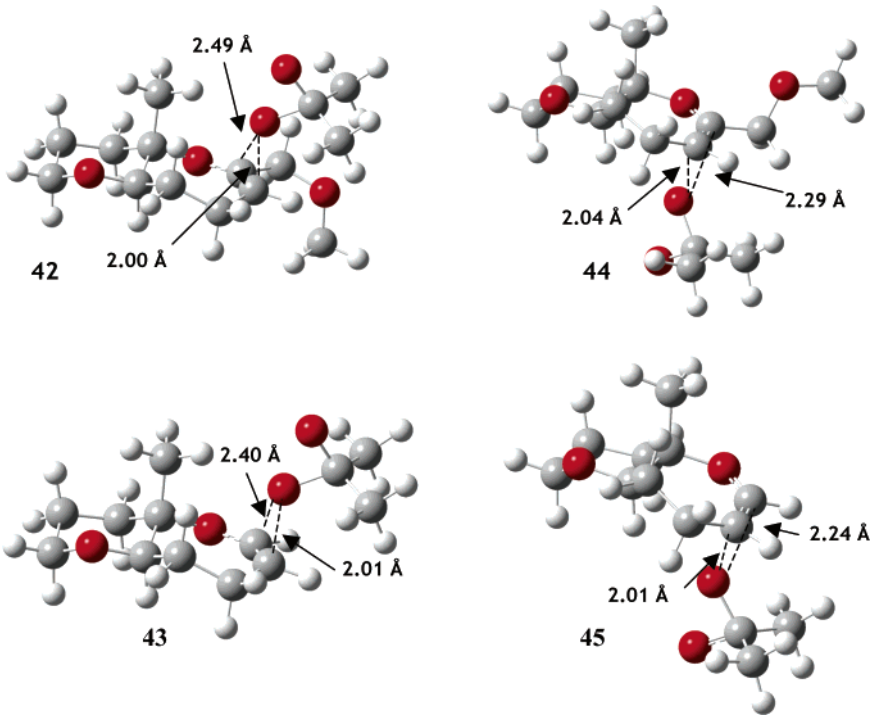

FIGURE 7. Calculated transition structures for the reaction of **36** and **37** with DMDO.

Inconsistent with this argument is that the relative energies of the less stable transition structures **44** and **45** are not affected by α-substitution. We currently believe that this is a consequence of other factors overriding the stabilization that would normally be observed with substitution. Namely, we surmise that the interactions between DMDO and the pseudoaxial allylic hydrogens dominate **44** and **45**. Consistent with this is that **44** and **45** are much less asynchronous than **42** and **43** and that they essentially have identical differences in their C(1) and C(2) C−O bond lengths.

Conclusion

In an attempt to better understand experimentally observed diastereoselectivity, we have computed transition states for the DMDO oxidation of a number of dihydropyrans and oxepenes using DFT methods and have found the calculations to be consistent with our experimental results. In all cases, the oxidations are asynchronous and proceed through the expected spiro-transition state. The degree of symmetry with respect to C−O bond formation appears to have an important effect on

the stereochemical outcome of the reactions especially when combined with unfavorable torsional interactions. In the dihydropyran oxidations, we believe that torsional strain between the C(3) substituent and DMDO dictate the stereoselectivity. In the oxepene reactions, we propose that the diastereoselectivity can be explained by increasing torsional strain between the newly formed C−O bond and the allylic pseudoaxial C−H bond in the disfavored transition structure. These results should help others and us in the use of cyclic enol ether oxidation chemistry in the generation of complex molecular systems.

Acknowledgment. We are grateful to NIGMS (Grant GM56677) for funding this work. The authors thank Mr. Paul Ha-Yeon Cheong from the Houk laboratory for helpful discussions. An allocation of computer time from the Center for High Performance Computing at the University of Utah is also gratefully acknowledged. Some of the computational resources used in this project were on the Arches Metacluster, administered by the University of Utah Center for High Performance Computing and funded by the National Institutes of Health (Grant No. NCRR 1 S10 RR17214-01).

Supporting Information Available: Cartesian coordinates of all optimized structures reported in this paper, the calculated energies and, in the case of the transition states, the imaginary frequency corresponding to the reaction coordinate, and the results of the IRC calculations on all transition states including plots of the energy and gradients along the reaction pathway. This material is available free of charge via the Internet at http://pubs.acs.org.

JO060502G